Fig. 2. *TLR7* SNP rs3853839 plays a functional role in TLR7 regulation. (*A*) Correlation of the *TLR7* transcript levels in PBMCs from Chinese individuals with rs3853839 genotypes. G represents the major allele and C represents the minor allele of rs3853839. Each symbol represents an individual, and horizontal lines indicate mean values. (*B*) Allelic specific transcriptional expression of *TLR7* in Chinese female subjects heterozygous for rs3853839 (G/C genotype) by pyrosequencing. *TLR7* transcripts containing risk G allele were significantly elevated in PBMCs compared with those containing C allele. (*C*) XCI analysis in Chinese female individuals was performed by measuring the degree of methylated CAG repeats in *AR* gene and revealed no significant skewing XCI among SLE cases (n = 21) and normal controls (n = 16). (*D*) Comparison of IFN signature in PBMCs from clinically inactive female patients with SLE carrying various genotypes using IFN score. IFN score was calculated by combination of mRNA expression levels of four IFN-regulated genes including *LY6E*, *MX1*, *IFIT1*, and *IFIT3* as described in *Materials and Methods*. Patients with SLE carrying GG genotype showed a more pronounced IFN signature in PBMCs compared with those carrying GC and CC genotypes.

autoimmunity (7). Whereas a modest increase in *TLR7* gene dosage promoted autoreactive lymphocytes with RNA specificities and myeloid cell proliferation, a substantial increase in *TLR7* expression caused fatal acute inflammatory pathologic process and profound dendritic cell dysregulation. In contrast, *TLR7*-deficient mice had ameliorated lupus disease, decreased lymphocyte activation, and decreased serum IgG (8). In addition, inhibitors of TLR7 reduced a number of lupus-associated phenotypes both in the MRL and NZB/W lupus-prone strains (12). Although a genomic duplication of *Tlr7* was associated with an increased severity of lupus-like disease in a murine model, the similar finding was not translated to humans with SLE. Using quantitative real-time PCR, a copy number variation (CNV) study in multiple ethnic groups showed that the CN of *TLR7* varied in patients with SLE and normal controls, but it was not significantly increased among

patients with SLE compared with controls (13). The lack of difference in *TLR7* CNV between human SLE and controls led us to explore functional SNPs in the current study.

Using a case-control design, we fine-mapped the *TLR7–TLR8* region and identified and replicated the association of the *TLR7* 3′ UTR SNP rs3853839 with SLE. The significant elevation of *TLR7* transcripts in PBMCs from individuals carrying G risk allele, along with the notable higher level of G allele-containing *TLR7* transcripts in heterozygous participants, supported a functional role rs3853839 played in the regulation of *TLR7*. The allelic specific expression analysis by pyrosequencing as we presented here is an accurate and valid approach that represents the biologically functional consequence of a certain SNP in vivo; without subjecting to various confounding factors frequently associated with in vitro assays, such as inappropriate reporter gene construct or cell

line chosen or lack of suitable condition or agonists applied (14). Further bioinformatic analysis based on current databases did not provide a clue on how the SNP regulates mRNA expression: rs3853839 is not located in the binding site of any transcriptional factors or miRNAs; neither is it in the AU-rich sequence that is usually involved in mRNA decay. The exact mechanism is therefore yet to be elucidated.

It is perplexing that the X-linked *TLR7* association does not explain the female dominance of SLE. The observed stronger male effect of rs385839 supports the notion that unique genetic predispositions might exist for male lupus. Given that both *Tlr7* duplication in *Yaa* mice and *TLR7* SNP rs3853839 in humans were preferably associated with male lupus, there might be potential epistasis between *TLR7* and male sex background. This is supported by previous observation of substantially lower IFN response in male versus female subjects upon TLR7 agonist stimulation (15, 16). The sex difference in *TLR7*-mediated response has been used to account for the finding of higher viral loads in men than women in early HIV infection (16) and might explain, at least in part, the increased severity of several infectious diseases in male subjects (17). The sex-specific effect demonstrated by *TLR7* SNP therefore might have implications that go beyond SLE. It would be interesting to investigate the contribution of *TLR7* polymorphism to other diseases with the *TLR7* pathway involved, especially in those with sex-specific incidence and manifestations.

To help exclude the possibility that the low LD of rs3853839 with neighboring SNPs is caused by CNV in this region, we used three independent methods including SYBR Green quantitative real-time PCR assay, PmeI pulsed-field gel electrophoresis (PFGE) and TaqI genomic Southern blot analyses to detect the existence of CNV at *TLR7-8* locus. Samples from 223 patients with SLE and 139 normal controls were tested by real-time PCR assay (Fig. S2 and *SI Materials and Methods*), and *TLR7–TLR8* CNVs were detected only in patients with SLE, at a frequency of less than 2% (one male patient had a two-copy variant of both *TLR7* and *TLR8*, one female patient had a one-copy variant of *TLR7*, and another female patient had a one-copy variant of *TLR8*; Fig. S3). The PmeI-PFGE and TaqI genomic Southern blot analyses performed among 250 subjects, including 203 female and 47 male subjects, with a total of 453 X chromosomes did not show physical evidence of structural variations at *TLR7–TLR8* locus (frequency less than 0.2%; Fig. S4 and *SI Materials and Methods*). Our results were consistent with two recent studies that used customized CGH platforms, which have reported no evidence of greater than a 5% frequency of *TLR7–TLR8* CNVs greater than approximately 500 bp in 19 HapMap trios of individuals of European descent from Utah, 20 HapMap trios from Yoruba individuals in Nigeria, 10 HapMap trios of Han Chinese individuals from Beijing, 10 HapMap trios of Japanese individuals from Tokyo, and 10 Korean female individuals, with an estimated statistical power of 95% (18, 19). Additionally, no structural variants at *TLR7–TLR8* locus have been described in the current Database of Genomic Variants (http://projects.tcag.ca/variation; RCh37, February 2009). Taken together, it is unlikely that the low LD between rs3853839 and neighboring SNPs is attributed to CNVs of this locus.

Currently, four European and two Asian genome-wide association studies (GWASs) in SLE have been published and more than 20 risk loci have been identified and replicated, which do not include the SLE-associated *TLR7* SNP described here (20–25). There are various factors that may influence the association detection in a GWAS, including sample size, study design, cohort demographics (ethnicity and sex composition, for example), analytical strategies, and in the case of rs3853839, SNP selection. Rs3853839, located in a region with poor LD structure, has not been included in commercial predesigned genotyping arrays, which could explain why the previous GWAS failed to capture this risk SNP. To estimate power of these GWAS to identify *TLR7* SNP association, we separately examined the male and female samples,

set the level of significance (*P* value) for the subsequent replication study in each GWAS, and assumed the associated allele G with an odds ratio of 1.79 in male subjects and 1.22 in female subjects (OR was identified in our discovery panel study). The power estimate for male samples is less than 1% in Asian GWASs and ranges between 2% and 7% in European GWASs, whereas for female samples it ranges between 1% and 3.4% in Asian GWASs and 3% and 24% in European GWASs. Thus, these studies have inadequate power to identify this *TLR7* association in their primary analyses. Our study was focused on the X chromosome; therefore, our correction for multiple testing was less stringent than the others that were conducted genome-wide, providing us greater power. In addition, fairly large sample size of male subjects with SLE and male controls (358 and 1,550, respectively, currently the largest male lupus study to our knowledge) facilitated our ability to detect the stronger effect of rs3853839 in male subjects. However, our male sample size is still not large enough to be comparable to female SLE genetic studies, and large-scale independent studies are needed to verify the effect of *TLR7* in men.

In summary, we identified a functional polymorphism in rs3853839 that may confer elevated expression of *TLR7* and predisposes to the development of SLE, especially in Chinese and Japanese male individuals. These data provide compelling evidence supporting a causal role for the type I IFN pathway genes in human autoimmunity and highlight the importance to explore sex-specific genetic contribution in a sex-biased disease such as SLE.

Materials and Methods

Clinical Samples. In the discovery panel, we genotyped 27 SNPs spanning the *TLR7* and *TLR8* gene region in 1,434 SLE cases and 1,591 controls of Eastern Asian ancestry. These samples were obtained from multiple centers in the United States and Eastern Asia, of which 563 cases and 522 controls were Chinese, 845 cases and 1,022 controls were Korean, and 26 cases and 47 controls were Japanese. The Chinese replication panel included 2,340 independent Chinese SLE cases and 2,436 controls, collected by collaborators in Shanghai (case vs. control: 687 vs. 849), Hong Kong (881 vs. 840), and Taiwan (772 vs. 747). The Japanese replication panel included 560 SLE cases and 913 controls that were recruited from two centers in Japan. All SLE cases fulfilled the 1997 revised American College of Rheumatology criteria for the classification of SLE (26). Informed consent was obtained from all subjects. The study was approved by the human subject institutional review boards and ethical committees at each of the participating locations.

SNP Selection and Genotyping. In the discovery panel, DNA from each subject was genotyped using custom-designed Beadstation Infinium II platform (Illumina). Genotyping was performed at the Lupus Genetics Studies Unit of the Oklahoma Medical Research Foundation. Twelve SNPs within *TLR7* and 15 SNPs within *TLR8* that either tagged major haplotypes in the HapMap database (January 2009) or were potentially functional were selected for genotyping. The average call rate for all samples was 98.3%. In the replication panels, rs3853839 and rs5935436 were genotyped by predesigned TaqMan SNP genotyping assay (Applied Biosystems) according to the manufacturer's instructions.

DNA Sequencing. We sequenced 5′ promoter region (up to 2 kb upstream) as well as three exons (including 3′UTR in exon 3) of *TLR7* in 48 Chinese female subjects. Briefly, consecutive overlapping amplicons were amplified from gDNA extracted from peripheral blood leukocytes. Primer pairs used are shown in Table S2.

Allelic Expression of TLR7 in PBMCs. The mRNA expression level of *TLR7* was measured in PBMCs from Chinese individuals carrying different genotypes of rs3853839. Briefly, total RNA was extracted from PBMCs using TRIzol (Invitrogen). RNA samples were then treated with DNase to eliminate gDNA contamination before being reverse-transcribed into cDNA. SYBR Green real-time PCR was used to measure the relative expression of *TLR7*. RPLP13A was used as internal control. We performed allelic-specific transcription quantification assay to measure the allelic expression of rs3853839 by using pyrosequencing as previously described (14). Ratios for each cDNA and gDNA from each individual was calculated by using PSQMA software (version 2.1; Biotage) and compared by paired Student *t* test.

15842 | www.pnas.org/cgi/doi/10.1073/pnas.1001337107

Shen et al.

— 136 —

IFN Signature in Patients with SLE. Expression levels of four type I IFN–regulated genes including *LY6E*, *MX1*, *IFIT1*, and *IFIT3* were measured by real-time PCR in PBMCs from female patients with SLE carrying various rs3853839 genotypes and normal controls. RPL13A was used as an internal control. The patients with SLE recruited in this part of study were in clinical remission defined by SLE Disease Activity Index 2000 (27) lower than 4 and prednisone dosage less than 15 mg/d. IFN scores were calculated as described in previous studies (10, 11).

XCI Analysis in Female Participants. We performed XCI analysis in female GC heterozygotes by measuring the degree of methylated CAG repeats in *AR* gene as previously described (9). Briefly, methylation-sensitive restriction enzyme HpaII was used to digest unmethylated (active X chromosome) DNA, which is thereby unable to amplify during the following PCR. Postdigestion PCR products therefore represent methylated (inactive X chromosome) DNA sequence. PCR products were sized using 5% denaturing polyacrylamide gel electrophoresis in an ABI Prism 3730 DNA automated sequencer, and analyzed by using Genescan Analysis 3.1 software (Applied Biosystems) as described previously (28).

Western Blot Analysis. Proteins were extracted from PBMCs of Chinese male controls carrying rs3853839 G and C allele (*n* = 6 and *n* = 2, respectively) to conduct Western blot analysis (*SI Materials and Methods*).

CNV Discovery Experiment. CNV discovery experiments are described in *SI Materials and Methods*. Study cohorts for CNV using real-time PCR assay and Southern blot analyses are shown in Tables S3 and S4, respectively.

Statistical Analysis. For single SNP analysis, we used gPLINK 1.062 software (http://pngu.mgh.harvard.edu/~purcell/plink/gplink.shtml) to evaluate the significance of differences in allelic frequencies of each SNP in the case-control samples. Bonferroni correction was used for multiple testing corrections in the discovery panel. For haplotype-based analysis, we used Haploview version 4.03 software (http://www.broad.mit.edu/mpg/haploview/index.php) to calculate pairwise LD indices R^2 and D', define LD blocks, infer haplotype frequencies, and analyze the significance of associations. We used the Q statistic (weighted sum of squares) to test the heterogeneity of odds ratio between male and female subsets. We used the Mann-Whitney test to compare the mRNA expression level of TLR7 in PBMCs from individuals carrying different genotypes. A paired Student *t* test was used to compare the G/C ratio between DNA and cDNA. A P value lower than 0.05 was considered to be statistically significant.

1. Rahman A, Isenberg DA (2008) Systemic lupus erythematosus. *N Engl J Med* 358: 929–939.
2. Yacoub Wasef SZ (2004) Gender differences in systemic lupus erythematosus. *Gend Med* 1:12–17.
3. Scofield RH, et al. (2008) Klinefelter's syndrome (47,XXY) in male systemic lupus erythematosus patients: Support for the notion of a gene-dose effect from the X chromosome. *Arthritis Rheum* 58:2511–2517.
4. Gilliet M, Cao W, Liu YJ (2008) Plasmacytoid dendritic cells: Sensing nucleic acids in viral infection and autoimmune diseases. *Nat Rev Immunol* 8:594–606.
5. Banchereau J, Pascual V (2006) Type I interferon in systemic lupus erythematosus and other autoimmune diseases. *Immunity* 25:383–392.
6. Pisitkun P, et al. (2006) Autoreactive B cell responses to RNA-related antigens due to TLR7 gene duplication. *Science* 312:1669–1672.
7. Deane JA, et al. (2007) Control of toll-like receptor 7 expression is essential to restrict autoimmunity and dendritic cell proliferation. *Immunity* 27:801–810.
8. Christensen SR, et al. (2006) Toll-like receptor 7 and TLR9 dictate autoantibody specificity and have opposing inflammatory and regulatory roles in a murine model of lupus. *Immunity* 25:417–428.
9. Allen RC, Zoghbi HY, Moseley AB, Rosenblatt HM, Belmont JW (1992) Methylation of HpaII and HhaI sites near the polymorphic CAG repeat in the human androgen-receptor gene correlates with X chromosome inactivation. *Am J Hum Genet* 51: 1229–1239.
10. Feng X, et al. (2006) Association of increased interferon-inducible gene expression with disease activity and lupus nephritis in patients with systemic lupus erythematosus. *Arthritis Rheum* 54:2951–2962.
11. Fu Q, et al. (2008) Association of elevated transcript levels of interferon-inducible chemokines with disease activity and organ damage in systemic lupus erythematosus patients. *Arthritis Res Ther* 10:R112.
12. Barrat FJ, Meeker T, Chan JH, Guiducci C, Coffman RL (2007) Treatment of lupus-prone mice with a dual inhibitor of TLR7 and TLR9 leads to reduction of autoantibody production and amelioration of disease symptoms. *Eur J Immunol* 37:3582–3586.
13. Kelley J, Johnson MR, Alarcón GS, Kimberly RP, Edberg JC (2007) Variation in the relative copy number of the TLR7 gene in patients with systemic lupus erythematosus and healthy control subjects. *Arthritis Rheum* 56:3375–3378.
14. Sun A, Ge J, Siffert W, Frey UH (2005) Quantification of allele-specific G-protein beta3 subunit mRNA transcripts in different human cells and tissues by Pyrosequencing. *Eur J Hum Genet* 13:361–369.
15. Berghöfer B, et al. (2006) TLR7 ligands induce higher IFN-alpha production in females. *J Immunol* 177:2088–2096.
16. Meier A, et al. (2009) Sex differences in the Toll-like receptor-mediated response of plasmacytoid dendritic cells to HIV-1. *Nat Med* 15:955–959.
17. Fish EN (2008) The X-files in immunity: Sex-based differences predispose immune responses. *Nat Rev Immunol* 8:737–744.
18. Conrad DF, et al., Wellcome Trust Case Control Consortium (2010) Origins and functional impact of copy number variation in the human genome. *Nature* 464: 704–712.
19. Park H, et al. (2010) Discovery of common Asian copy number variants using integrated high-resolution array CGH and massively parallel DNA sequencing. *Nat Genet* 42:400–405.
20. Graham RR, et al. (2008) Genetic variants near TNFAIP3 on 6q23 are associated with systemic lupus erythematosus. *Nat Genet* 40:1059–1061.
21. Han JW, et al. (2009) Genome-wide association study in a Chinese Han population identifies nine new susceptibility loci for systemic lupus erythematosus. *Nat Genet* 41: 1234–1237.
22. Harley JB, et al., International Consortium for Systemic Lupus Erythematosus Genetics (SLEGEN) (2008) Genome-wide association scan in women with systemic lupus erythematosus identifies susceptibility variants in ITGAM, PXK, KIAA1542 and other loci. *Nat Genet* 40:204–210.
23. Han JW, et al. (2008) Association of systemic lupus erythematosus with C8orf13-BLK and ITGAM-ITGAX. *N Engl J Med* 358:900–909.
24. Kozyrev SV, et al. (2008) Functional variants in the B-cell gene BANK1 are associated with systemic lupus erythematosus. *Nat Genet* 40:211–216.
25. Yang W, et al., Asian Lupus Genetics Consortium (2010) Genome-wide association study in Asian populations identifies variants in ETS1 and WDFY4 associated with systemic lupus erythematosus. *PLoS Genet* 6:e1000841.
26. Hochberg MC (1997) Updating the American College of Rheumatology revised criteria for the classification of systemic lupus erythematosus. *Arthritis Rheum* 40: 1725.
27. Gladman DD, Ibañez D, Urowitz MB (2002) Systemic lupus erythematosus disease activity index 2000. *J Rheumatol* 29:288–291.
28. Lappalainen S, Utriainen P, Kuulasmaa T, Voutilainen R, Jääskeläinen J (2008) Androgen receptor gene CAG repeat polymorphism and X-chromosome inactivation in children with premature adrenarche. *J Clin Endocrinol Metab* 93:1304–1309.

New epitopes and function of anti-M3 muscarinic acetylcholine receptor antibodies in patients with Sjögren's syndrome

H. Tsuboi, I. Matsumoto,
E. Wakamatsu, Y. Nakamura,
M. Iizuka, T. Hayashi, D. Goto, S. Ito
and T. Sumida
Division of Clinical Immunology, Doctoral
Program in Clinical Sciences, Graduate School of
Comprehensive Human Sciences, University of
Tsukuba, Ibaraki, Japan

Summary

M3 muscarinic acetylcholine receptor (M3R) plays a crucial role in the secretion of saliva from salivary glands. It is reported that some patients with Sjögren's syndrome (SS) carried inhibitory autoantibodies against M3R. The purpose of this study is to clarify the epitopes and function of anti-M3R antibodies in SS. We synthesized peptides encoding the extracellular domains of human-M3R including the N-terminal region and the first, second and third extracellular loops. Antibodies against these regions were examined by enzyme-linked immunosorbent assay in sera from 42 SS and 42 healthy controls. For functional analysis, human salivary gland (HSG) cells were preincubated with immunoglobulin G (IgG) separated from sera of anti-M3R antibody-positive SS, -negative SS and controls for 12 h. After loading with Fluo-3, HSG cells were stimulated with cevimeline hydrochloride, and intracellular Ca^{2+} concentrations [(Ca^{2+})i] were measured. Antibodies to the N-terminal, first, second and third loops were detected in 42·9% (18 of 42), 47·6% (20 of 42), 54·8% (23 of 42) and 45·2% (19 of 42) of SS, while in 4·8% (two of 42), 7·1% (three of 42), 2·4% (one of 42) and 2·4% (one of 42) of controls, respectively. Antibodies to the second loop positive SS-IgG inhibited the increase of (Ca^{2+})i induced by cevimeline hydrochloride. Antibodies to the N-terminal positive SS-IgG and antibodies to the first loop positive SS-IgG enhanced it, while antibodies to the third loop positive SS-IgG showed no effect on (Ca^{2+})i as well as anti-M3R antibody-negative SS-IgG. Our results indicated the presence of several B cell epitopes on M3R in SS. The influence of anti-M3R antibodies on salivary secretion might differ based on these epitopes.

Keywords: autoantibodies, epitopes, function, M3 muscarinic acetylcholine receptor, Sjögren's syndrome

Introduction

Sjögren's syndrome (SS) is an autoimmune disease that affects exocrine glands, including salivary and lacrimal glands. It is characterized by lymphocytic infiltration into exocrine glands, leading to dry mouth and eyes. A number of autoantibodies, such as anti-SS-A and SS-B antibodies, are detected in patients with SS. However, no SS-specific pathological autoantibodies have yet been found in this condition [1].

Data from recent studies have suggested that some patients with SS carry inhibitory autoantibodies directed against muscarinic acetylcholine receptors, especially M3 muscarinic acetylcholine receptor (M3R) [1]. To date, five

subtypes of muscarinic acetylcholine receptors (M1R–M5R) have been identified, and M3R is expressed in exocrine glands and plays crucial roles in exocrine secretion. Acetylcholine binds to and activates M3R on salivary gland cells, causing a rise in intracellular Ca^{2+} via inositol 1, 4, 5-trisphosphate (IP3) and IP3 receptors. Consequently, the rise in intracellular Ca^{2+} activates apical membrane Cl^- channels and induces salivary secretion [1]. Activation of M3R also induces trafficking of aquaporin 5 (AQP5) to the apical membrane from the cytoplasm, which causes rapid transport of water across the cell membrane [2]. M3R has four extracellular domains: the N-terminal region and the first, second and third extracellular loops. Among these domains, the second extracellular loop is critical for receptor

activation by agonists [3]. Therefore, the second extracellular loop of M3R has been the focus of our interest, and we report a subgroup of SS patients who had anti-M3R antibodies that recognized the second extracellular loop of M3R [4,5]. Although these data indicate that the second extracellular loop is the target antigen, the precise epitopes are currently unknown. A recent study reported that the third extracellular loop represents a functional epitope bound by IgG derived from SS patients [6].

The present study was designed to clarify the precise B cell epitopes of M3R and the function of anti-M3R antibodies. For this purpose, we screened sera of SS patients for anti-M3R autoantibodies against all four extracellular domains of M3R by enzyme-linked immunosorbent assay (ELISA) using synthetic peptide antigens and performed functional assays of these antibodies using human salivary gland (HSG) cells. We assessed the correlation between epitopes and function and various clinical features.

Materials and methods

Study population

Serum samples were collected from 42 Japanese patients with SS (15 with primary SS and 27 with secondary SS) who had been followed-up at the Division of Rheumatology, University of Tsukuba Hospital, Ibaraki, Japan. All patients with SS satisfied the Japanese Ministry of Health criteria for the diagnosis of SS. These criteria included four clinicopathological findings: lymphocytic infiltration of the salivary or lacrimal glands, dysfunction of salivary secretion, keratoconjunctivitis sicca and presence of anti-SS-A or SS-B antibodies. The diagnosis of SS was based on the presence of two or more of the above items. We also recruited 42 healthy controls (HC). Approval for this study was obtained from the local ethics committee and signed informed consent was obtained from each subject.

Synthesis of peptide antigens

We synthesized different peptides encoding the extracellular domains of human-M3R. The N-terminal of human-M3R has a 66-mer amino acid sequence, and accordingly we divided this domain into three segments. The sequences were: MTLHNNSTTSPLFPNISSSWIHSPSDAGLP for N-terminal 1, IHSPSDAGLPPGTVTHFGSYNVSRAAGNFS for N-terminal 2 and NVSRAAGNFSSPDGTTDDPLGGHT VWQV for N-terminal 3 (Sigma-Aldrich Japan, Ishikari, Japan). These three peptides were mixed and used for the peptide antigens of the N-terminal region. We also synthesized three peptides corresponding to the sequences of the three extracellular loops of human-M3R, the sequences of which were FTTYIIMNRWALGNLACDLW for the first extracellular loop, KRTVPPGECFIQFLSEPTITFGTAI for the second and VLVNTFCDSCIPKTFWNLGY for the third

(Sigma-Aldrich Japan). As a control peptide, we synthesized a peptide corresponding to the sequences of the third extracellular loop of human-M5 muscarinic acetylcholine receptor (M5R), the sequences of which were STFCD-KCVPVTLWH (Sigma-Aldrich Japan). As a negative peptide, we also synthesized a 25-mer peptide whose sequence was SGSGSGSGSGSGSGSGSGSGSGSGS (Sigma-Aldrich Japan).

ELISA

Peptide solution (100 µl/well at 10 µg/ml) in 0·1 M Na_2CO_3 buffer, pH 9·6, was adsorbed onto a Nunc-Immuno plate (Nalge Nunc International, Rochester, NY, USA) overnight at 4°C, and blocked with 5% bovine serum albumin (NSA) (Wako Pure Chemical Industries, Osaka, Japan) in phosphate-buffered saline (PBS) for 1 h at 37°C. For the dose-dependent curve, serum from anti-M3R antibodies positive SS and from HC diluted at 1:25, 1:50, 1:100, 1:200, 1:400, 1:800 and 1:1600 in blocking buffer, and incubated for 2 h at 37°C. Serum to be examined at 1:50 dilution in blocking buffer was also incubated for 2 h at 37°C. The plates were then washed six times with 0·05% Tween20 in PBS, and 100 µl of solution of alkaline phosphatase-conjugated goat anti-human IgG (Fc; American Qualex, San Clemente, CA, USA) diluted 1:1000 in PBS was added for 1 h at room temperature. After nine washes, 100 µl of p-nitrophenyl phosphate (Sigma) solution was added at a final concentration of 1 mg/ml as alkaline phosphatase substrate. Plates were incubated for 30 min at room temperature in the dark, and the absorbance at 405 nm was measured by plate spectrophotometry. Measurements were performed in triplicate and standardized between experiments by using the absorbance value of the positive control.

Measurement of salivary secretion

We assessed salivary secretion by the gum test. In this test, the volume of saliva is measured after chewing gum for 10 min.

Histopathological examination

Histopathological findings of the labial salivary glands were classified according to Greenspan grading [7].

Expression of M3R mRNA in HSG cells

Total RNA was extracted from HSG cells and cDNA was synthesized by cDNA synthesis kit (Fermentas International, Burlington, Ontario, Canada). Polymerase chain reaction (PCR) was performed with cDNA using the human-M3R-specific primers [2]. The human glyceraldehyde-3-phosphate dehydrogenase (GAPDH) was amplified to assess the cDNA yield.

Expression of M3R proteins on the cell surface of HSG cells

For immunofluorescent analysis, HSG cells were precultured in two-well chamber slides for 48 h. Without fixation, HSG cells were incubated with the first antibodies: anti-human M3R antibody (goat IgG, polyclonal; Santa Cruz Biotechnology, Santa Cruz, CA, USA) or goat control IgG (Invitrogen Corporation, Carlsbad, CA, USA) for 2 h. After washing, HSG cells were incubated with the second antibodies: fluorescein isothiocyanate (FITC)-conjugated rabbit anti-goat IgG antibodies (IgG; MP Biomedicals, Irvine, CA, USA). Stained HSG cells were observed by fluorescence microscope.

Functional assays

HSG cells (15 000 cells/well) were precultured in 96-well plates for fluorescence assays at 37°C for 48 h. Then, the cells were preincubated with IgG fractions separated from sera of anti-M3R antibodies positive for five SS patients, anti-M3R antibodies negative for one SS patient, and HC by using protein G column (1·0 mg/ml) for 12 h. The referral of the anti-M3R antibodies positive or negative sera was on the basis of our ELISA results. IgG was washed off and the HSG cells were loaded with Fluo-3, which was a fluorescence probe for calcium, for 1 h. Fluo-3 was washed off, and then the Ca²⁺ influx assay, the HSG cells were stimulated with cevimeline hydrochloride, which was a M3R specific agonist at a final concentration of 20 mM. Changes in intracellular calcium concentrations [(Ca²⁺)i] in HSG cells were measured by fluorescence plate reader. Maximum changes of (Ca²⁺)i [peak (Ca²⁺)i – baseline (Ca²⁺)i] in IgG from SS patients or without IgG were shown as ratiometric data compared to maximum change of (Ca²⁺)i in HC [2].

Statistical analysis

Differences between groups were examined for statistical significance using the Mann–Whitney U-test, while differences in frequencies were analysed by Fisher's exact probability test. A P-value less than 0·05 was considered as the statistically significant difference.

Results

Anti-M3R antibodies in patients with SS and control subjects

The average age of SS patients was 53·1 ± 13·2 years, that of HC was 33·1 ± 8·7 years (P < 0·05, Mann–Whitney U-test). All 42 SS patients were female, 22 of HC female and 20 of HC male. Among 27 patients with secondary SS, 11 were complicated with rheumatoid arthritis (RA), 11 with systemic lupus erythematosus (SLE), two with mixed connective tissue disease (MCTD) and three with other autoimmune diseases.

Anti-M3R antibodies were really specific for each M3R peptide, because the binding activities of sera from SS patients were dose-dependent and were not in the control sera from healthy subjects. Furthermore, sera from anti-M3R antibodies positive SS did not recognize the peptide corresponding to the sequences of the third extracellular loop of human-M5R (Fig. 1a).

Antibodies to the N-terminal region were detected in 42·9% (18 of 42) of SS patients but in only 4·8% (two of 42) of the control (P < 0·05, Fisher's exact probability test). Antibodies to the first extracellular loop were detected in 47·6% (20 of 42) of SS and 7·1% (three of 42) of the control (P < 0·05, Fisher's exact probability test). Antibodies to the second extracellular loop were detected in 54·8% (23 of 42) of SS and 2·4% (one of 42) of the control (P < 0·05, Fisher's exact probability test). Antibodies to the third extracellular loop were detected in 45·2% (19 of 42) of SS and 2·4% (one of 42) of the control (P < 0·05, Fisher's exact probability test). The frequencies and titres of anti-M3R antibodies against all extracellular domains were significantly higher in SS patients than the control (P < 0·05, Fisher's exact probability test for frequencies, Mann–Whitney U-test for titres) (Fig. 1b).

B cell epitopes on the M3R

Table 1 lists the epitopes of anti-M3R antibodies in patients with SS. Of the 42 SS patients, 28 had anti-M3R antibodies reactive to at least one B cell epitope on the M3R, while the other 14 SS patients did not have any anti-M3R antibodies. Antibodies to one B cell epitope on the M3R (N-terminal, first, second and third extracellular loops) were detected in one, two, two and one of 28 SS patients, respectively. Antibodies reactive to two B cell epitopes (N-terminal and first extracellular loop, N-terminal and second extracellular loop, first and second extracellular loop, second and third extracellular loop) were detected in one, one, two and two SS patients, respectively. Two SS patients showed the presence of antibodies to three B cell epitopes (N-terminal and second and third extracellular loop, first and second and third extracellular loop). In 50% of the SS patients (14 of 28), antibodies reactive to all four B cell epitopes were detected. Based on these results, we concluded that anti-M3R antibodies had several B cell epitopes on the extracellular domains of M3R, and that some SS patients carried anti-M3R antibodies that recognized several extracellular domains of M3R.

Correlation between anti-M3R antibodies and various clinicopathological features

Disease duration of SS was shorter among anti-M3R antibody-positive SS (7·3 ± 7·6 years) than -negative SS

(a) N / 1st / 2nd / 3rd — graphs of ΔAbsorbance vs Dilution rate.

(b) N / 1st / 2nd / 3rd — scatter plots of ΔAbsorbance for SS and C.

N: Mean+2s.d. of the control = 0·074, $P < 0.05$

1st: Mean+2s.d. of the control = 0·141, $P < 0.05$

2nd: Mean+2s.d. of the control = 0·103, $P < 0.05$

3rd: Mean+2s.d. of the control = 0·145, $P < 0.05$

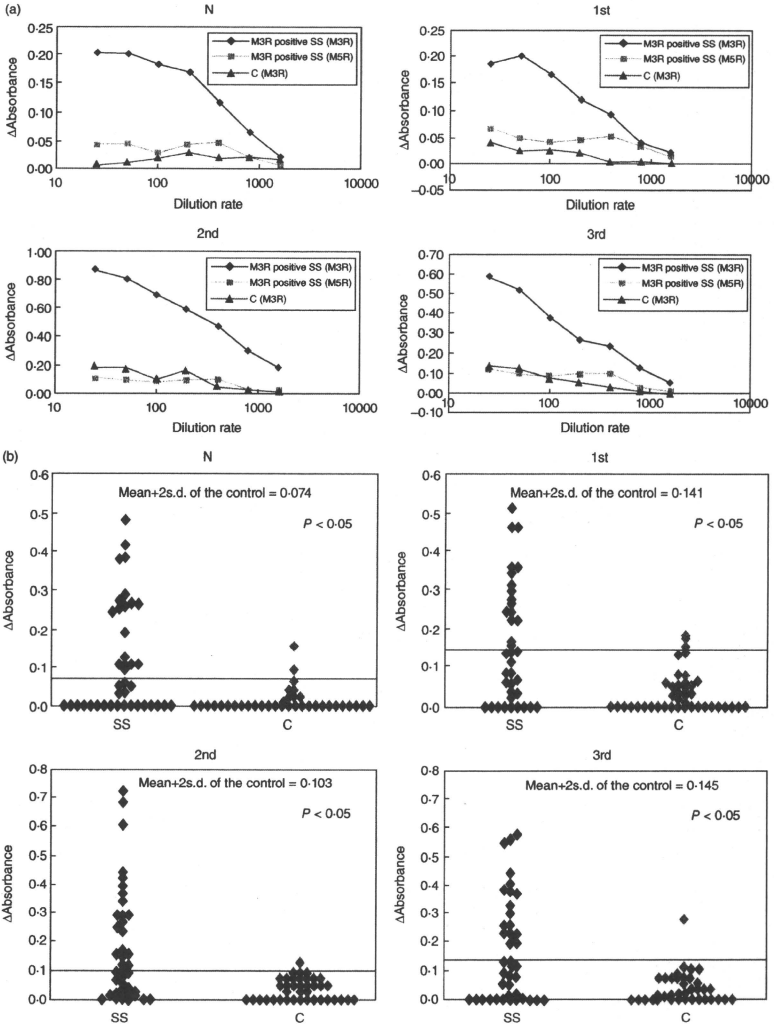Legends: M3R positive SS (M3R); M3R positive SS (M5R); C (M3R)

Fig. 1. (a) The dose-dependent curve on anti-M3 muscarinic acetylcholine receptor (M3R) antibodies. M3R and M5R peptide-specific absorbance values at 405 nm (Δabsorbance) were calculated for each serum sample by subtracting the absorbance value of the negative peptide from that of the peptides encoding the extracellular domains of human-M3R and M5R. The clear dose–response of M3R peptide-specific absorbance to changes on serum concentrations was shown in serum from anti-M3R antibody-positive Sjögren's syndrome (SS), but not in serum from healthy controls (C). The clear dose–response of the third extracellular loop of M5R-specific absorbance to changes on serum concentrations was not shown in serum from anti-M3R antibody-positive SS. (b) Anti-M3R antibodies in patients with SS and control subjects. M3R peptide-specific absorbance values at 405 nm (Δabsorbance) in Sjögren's syndrome (SS) and healthy controls (C). The cut-off level between negative and positive values was the mean ± 2 standard deviation value of the normal control (grey line). The prevalence and titres of anti-M3R antibodies against all extracellular domains were significantly higher in patients with SS than control subjects (Fisher's exact probability test for prevalence, Mann–Whitney U-test for titres). N: N-terminal region; 1st: first extracellular loop; 2nd: second extracellular loop; 3rd: third extracellular loop.

(15·5 ± 11·1 years, $P < 0.05$, Mann–Whitney U-test). The positivity for anti-SS-A antibody and the IgG value in serum was more prevalent and higher among anti-M3R antibody-positive SS than -negative SS ($P < 0.05$, Fisher's exact probability test and Mann–Whitney U-test). In contrast, there were no differences in age, positivity for anti-SS-B antibody and rheumatoid factor, tear volume by Schirmer test, saliva volume by gum test, extra-glandular involvement and Greenspan grading between anti-M3R antibody-positive

and -negative SS (Table 2). There is no significant relationship between each B cell epitope and clinical characteristics such as saliva secretion.

Expression of M3R mRNA and proteins in HSG cells

PCR products revealed the expression of M3R mRNA in HSG cells used in the present study. The expected PCR product for M3R was detected at 201 base pairs (bp)

Table 1. B cell epitopes on the M3 muscarinic acetylcholine receptor (M3R).

Number of B cell epitopes on the M3R	B cell epitopes on the M3R				Number of cases
	N	1st	2nd	3rd	
1	+	–	–	–	1
	–	+	–	–	2
	–	–	+	–	2
	–	–	–	+	1
2	+	+	–	–	1
	+	–	+	–	1
	–	+	+	–	2
	–	–	+	+	2
3	+	–	+	+	1
	–	+	+	+	1
4	+	+	+	+	14
Total number of cases					28

N, N-terminal; 1st, first extracellular loop; 2nd, second extracellular loop; 3rd, third extracellular loop; +, positive for anti-M3R antibodies; –, negative for anti-M3R antibodies.

Table 2. Clinicopathological features in anti-M3 muscarinic acetylcholine receptor (M3R) antibody-positive and -negative Sjögren's syndrome (SS) patients.

|	Positive SS $n = 28$	Negative SS $n = 28$	P-value
Primary/secondary	12/16	3/11	n.s.
Age (years)	51·4 ± 12·1	56·4 ± 12·1	n.s.
Disease duration (years)	7·3 ± 7·6	15·5 ± 11·1	$P < 0.05$
Anti-SSA (%)	92·9	57·1	$P < 0.05$
Anti-SSB (%)	21·4	14·3	n.s.
Rheumatoid factor (%)	46·4	50·0	n.s.
IgG (mg/dl)	2013 ± 767	1427 ± 515	$P < 0.05$
Extra-glandular involvements in primary SS (%)	83·3	66·7	n.s.
Schirmer test (mm/5 min)	4·4 ± 6·2	4·2 ± 5·0	n.s.
Gum test (ml/10 min)	8·3 ± 7·8	8·8 ± 5·1	n.s.
Histological examination (Greenspan grading)	3·1 ± 0·5	3·0 ± 0·8	n.s.

n.s., not statistically significant.
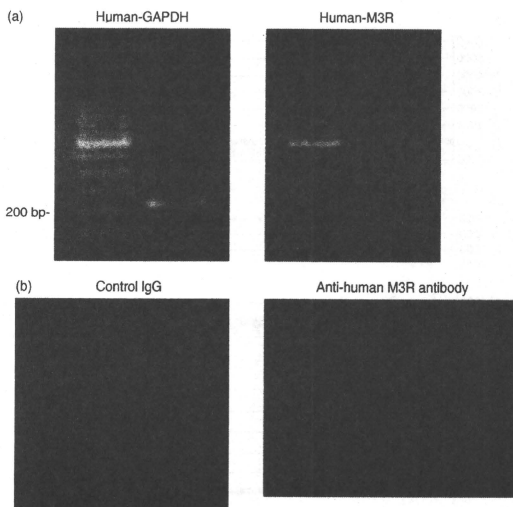
Fig. 2. (a) Expression of M3 muscarinic
acetylcholine receptor (M3R) mRNA in human
salivary gland (HSG) cells. (b) Expression of
M3R proteins on the surface of HSG cells
detected by immunofluorescent analysis.

(Fig. 2a). Moreover, M3R proteins were detected on HSG cells stained with anti-human M3R antibody, whereas they were not found with control IgG (Fig. 2b). These results indicated that HSG cells expressed M3R molecules on their surface.

Functional roles of anti-M3R antibodies

IgG derived from two SS patients positive for anti-M3R antibodies to the second extracellular loop inhibited the increase in $(Ca^{2+})i$ induced by cevimeline hydrochloride 16% and 25%, respectively ($P < 0.05$, *versus* IgG derived from HC, Mann–Whitney U-test) (Figs 3c,d and 4). In contrast, IgG derived from SS patients positive for antibodies to the N-terminal and the first extracellular loop enhanced the increase in $(Ca^{2+})i$ induced by cevimeline hydrochloride 14% and 15%, respectively ($P < 0.05$, *versus* IgG derived from HC, Mann–Whitney U-test) (Figs 3a,b and 4). IgG derived from a SS patient positive for antibodies to the third extracellular loop had no effect on $(Ca^{2+})I$, as well as IgG derived from an anti-M3R antibody-negative SS patient (Figs 3e and 4).

Discussion

Recently, anti-M3R antibodies have been the focus of interest in rheumatology because of their potential pathogenic role, use as diagnostic markers and being therapeutic targets in patients with SS [1]. Several methods have been used to

detect anti-M3R antibodies in SS patients [1]. In functional assays using smooth muscles, IgG fractions from patients with SS (SS-IgG) inhibited carbachol-evoked or nerve-evoked bladder or colon contractions [8,9]. In salivary gland cells, SS-IgG inhibited the rise in $(Ca^{2+})i$ induced by carbachol, and also inhibited pilocarpine-induced AQP5 trafficking to the apical membrane from the cytoplasm [2]. The inhibitory actions of SS-IgG on the rise in $(Ca^{2+})i$ was acutely reversible [10]. Anti-M3R antibodies from SS patients can be detected by immunofluorescent analysis using rat lacrimal glands [11], and by flow cytometry using the M3R-transfected Chinese hamster ovary (CHO) cell line [12]. Moreover, anti-M3R antibodies in sera of SS patients were detected by ELISA using synthetic peptides or recombinant proteins of the second extracellular loop of M3R [13]. We have reported previously the presence of anti-M3R antibodies in a group of patients with SS, which recognized the second extracellular loop by ELISA using synthetic peptides [4,5].

In the present study, we established a standard method to detect anti-M3R antibodies that can be used for screening large patient populations. Functional assays and flow cytometry are too laborious for routine use. Although ELISA is easy, the results from some ELISA systems used for screening anti-M3R antibodies differ widely with regard to the prevalence of anti-M3R antibodies (from 11 to 90%) [4,14]. Furthermore, Cavill *et al.* [15] reported failure to detect anti-M3R antibodies by ELISA using synthetic peptides. In the
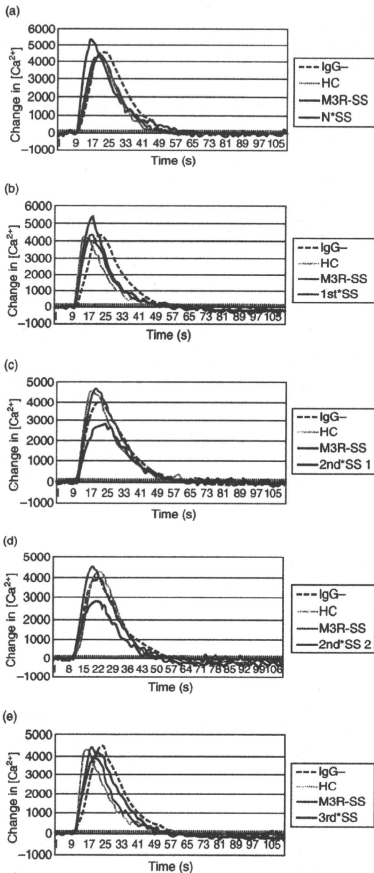
(a)

(b)

(c)

(d)

(e)

Fig. 3. Functional analysis of anti-M3 muscarinic acetylcholine receptor (M3R) antibodies in Sjögren's syndrome (SS) patients. (a,b) Immunoglobulin G (IgG) derived from SS patient with anti-M3R antibodies to the N-terminal region and the first extracellular loop enhanced the increase in (Ca^{2+})i induced by cevimeline hydrochloride 14% and 15%, respectively, compared to IgG from healthy control (HC). The traces were representative traces, which were performed in triplicate, and three independent experiments with each IgG. Human salivary gland (HSG) cells were stimulated with cevimeline hydrochloride (20 mM) at 10 s. IgG; without IgG, HC; IgG derived from healthy control, M3R·SS; IgG derived from SS patient negative for anti-M3R antibodies, N⁺SS; IgG derived from SS patient positive for anti-M3R antibodies to the N-terminal region; 1st⁺SS; IgG derived from SS patient positive for anti-M3R antibodies to the first extracellular loop. (c,d) IgG derived from two SS patients positive for antibodies to the second extracellular loop inhibited the increase in (Ca^{2+})i induced by cevimeline hydrochloride 16% and 25%, respectively, compared to IgG from HC. The traces were representative traces, which were performed in triplicate, and three independent experiments with each IgG; 2nd⁺SS: IgG derived from SS patient positive for anti-M3R antibodies to the second extracellular loop. (e) IgG derived from SS patient positive for antibodies to the third extracellular loop had no effect on the increase in (Ca^{2+})i induced by cevimeline hydrochloride. The traces were representative traces, which were performed in triplicate, and three independent experiments with each IgG; 3rd⁺SS: IgG derived from SS patient positive for antibodies to the third extracellular loop.

◄

present study, we reported higher frequencies and titres of anti-M3R antibodies against all extracellular domains in SS patients than the control. The prevalence of anti-M3R antibodies against the second extracellular loop in SS (55%) determined in the present study was much higher than that reported in our previous study (11%) [4]. The reason for this difference is probably related to the change in the methodology, such as increased sensitivity resulting from purity of the synthetic peptides, modification of the washing

procedure or other factors introduced in the modified ELISA system.

In the present study, we also determined the precise B cell epitopes of M3R molecules. B cell epitopes in the present study are areas including peptides recognized by anti-M3R antibodies, although we do not know whether or not these linear peptides are really conformational epitopes. However, we showed that anti-M3R antibodies against these linear epitopes exactly influenced Ca influx via M3R in HSG cells. Therefore, we suggest that these linear peptides might consist of the conformational epitopes on the M3R. Several B cell epitopes were identified on the extracellular domains, and some SS patients were reactive to several extracellular domains other than the second extracellular loop. The second extracellular loop of M3R has been the focus of our interest in epitopes and function of anti-M3R antibodies [4,5,9,10]. Recently, Koo *et al.* [6] reported that the third extracellular loop represents a functional epitope bound by SS-IgG. In contrast to these results, we found in the present study that antibodies to the second extracellular loop of M3R inhibited the increase of (Ca^{2+})i induced by cevimeline hydrochloride in a functional assay using HSG cells. This inhibitory effect of anti-M3R antibodies might explain the reduction in salivary secretion in some SS patients. Our data also demonstrated that antibodies against the third extracellular loop did not have an effect on the increase in (Ca^{2+})i, while antibodies against the N-terminal and first extracellular loop enhanced the increase in (Ca^{2+})i. These results
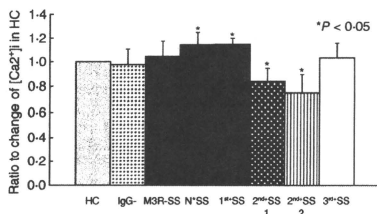
59

Fig. 4. Summary of B cell epitopes on M3 muscarinic acetylcholine receptor (M3R) and the function of anti-M3R antibodies in Sjögren's syndrome (SS) patients. Mean ± standard deviation values of maximum change in $(Ca^{2+})i$ [peak $(Ca^{2+})i - (Ca^{2+})i$] induced by cevimeline hydrochloride in immunoglobulin G (IgG) from SS patients or without IgG were shown as a ratio compared to maximum change of $(Ca^{2+})i$ in healthy control (HC). The maximum change in HC was described as 1·0. Data were averaged of triplicate and three independent experiments. *$P < 0.05$ versus IgG derived from HC, Mann–Whitney U-test, HC, IgG⁻, M3R⁻SS, N⁺SS, 1st⁺SS, 2nd⁺SS and 3rd⁺SS; the same as in Fig. 3.

indicate that the effects of anti-M3R antibodies on the secretion of saliva could be different from these epitopes, although further experiments using antibodies from more patients are necessary.

Although the molecular mechanisms on the difference among individual B cell epitopes have not been elucidated, we could propose the following three possibilities. The first is that antibodies against the second extracellular domain of M3R directly inhibit the intracellular signal pathway, resulting in the decrease of Ca^{2+} influx and reduction of saliva. In contrast, antibodies against N-terminal region and the first extracellular domain of M3R might enhance the intracellular signalling and increase of Ca^{2+} influx. The second is that anti-M3R antibodies binding to the second extracellular domain could inhibit the M3R agonist, and then antibodies suppress indirectly the stimulation of Ca^{2+} influx. The third is that anti-M3R antibodies influence the expression of M3R molecules on HSG. Some antibodies which target the N-terminal region or the first extracellular loop of M3R may be able to up-regulate expression of M3R and enhance Ca^{2+} influx, whereas the other antibodies against the second extracellular domain might down-regulate the expression of M3R on HSG, resulting in a reduction of Ca^{2+} influx. It has been reported that the expression of M3R in salivary glands could be affected by anti-M3R antibodies in patients with SS [1]. Further experiments on the effect of anti-M3R antibodies on M3R signalling, binding to the M3R agonist, and the influence on M3R expression should shed light on the mechanism of the different functions of anti-M3R antibodies.

We have reported previously the presence of anti-M3R antibodies that recognized the second extracellular loop in SS patients but not in patients with RA or SLE, suggesting that anti-M3R antibodies could be used potentially as diagnostic markers for SS [4]. However, Kovacs et al. [14] reported the detection of anti-M3R antibodies in 35% of their RA patients and 32% of SLE. These conflicting results emphasize the need to examine the precise prevalence of anti-M3R antibodies in other autoimmune diseases using our modified ELISA system.

The correlation between anti-M3R antibodies and clinical features is still unclear. The previous study reported leukopenia was more common in anti-M3R antibody-positive than in -negative patients with primary SS [14]. Our observations in the present study showed that positivity for anti-SS-A antibody and IgG values in serum was more prevalent and higher in anti-M3R antibody-positive SS patients than -negative SS patients. The disease duration of SS was shorter among anti-M3R antibody-positive SS than -negative SS; however, there was no difference in other clinical and histological features between anti-M3R antibody-positive and -negative SS patients. We could not detect any significant relationship between each B cell epitope and clinical characteristics such as saliva secretion.

In conclusion, these findings support the notion of presence of several B cell epitopes on M3R in SS patients, and that some SS patients are reactive to several extracellular domains of the M3R. It is possible that some anti-M3R antibodies alter salivary secretion in SS via M3R, and in particular antibodies against the second extracellular loop of the M3R could suppress the increase in $(Ca^{2+})i$ induced by M3R agonists, resulting in reduction of salivary secretion. Therefore, anti-M3R antibodies might play pathogenic roles in salivary secretion abnormalities characteristic of patients with SS.

Disclosure

None of the authors has any conflict of interest with the subject matter or materials discussed in the manuscript.

References

1 Dawson L, Tobin A, Smith P, Gorton T. Antimuscarinic antibodies in Sjögren's syndrome. Arthritis Rheum 2005; 52:2984–95.

2 Li J, Ha YM, Ku NY et al. Inhibitory effects of autoantibodies on the muscarinic receptors in Sjögren's syndrome. Lab Invest 2004; 84:1430–8.

3 Scarselli M, Li B, Kim SK, Wess J. Multiple residues in the second extracellular loop are critical for M3 muscarinic acetylcholine receptor activation. J Biol Chem 2007; 282:7385–96.

4 Naito Y, Matsumoto I, Wakamatsu E et al. Muscarinic acetylcholine receptor autoantibodies in patients with Sjögren's syndrome. Ann Rheum Dis 2005; 64:510–11.

5 Nakamura Y, Wakamatsu E, Matsumoto I et al. High prevalence of autoantibodies to muscarinic-3 acetylcholine receptor in patients with juvenile-onset Sjögren's syndrome. Ann Rheum Dis 2008; 67:136–7.

6 Koo NY, Li J, Hwang SM *et al.* Functional epitopes of muscarinic type3 receptor which interacts with autoantibodies from Sjögren's syndrome patients. Rheumatology 2008; 47:828–33.

7 Greenspan JS, Daniels TE, Talal N, Sylvester RA. The histopathology of Sjögren's syndrome in labial salivary gland biopsies. Oral Surg Oral Med Oral Pathol 1974; 37:217–29.

8 Waterman SA, Gordon TP, Rischmueller M. Inhibitory effects of muscarinic receptor autoantibodies on parasympathetic neurotransmission in Sjögren's syndrome. Arthritis Rheum 2000; 43:1647–54.

9 Cavill D, Waterman SA, Gordon TP. Antibodies raised against the second extracellular loop of the human muscarinic M3 receptor mimic functional autoantibodies in Sjögren's syndrome. Scand J Immunol 2004; 59:261–6.

10 Dawson LJ, Stanbury J, Venn N, Hasdimir B, Rogers SN, Smith PM. Antimuscarinic antibodies in primary Sjögren's syndrome reversibly inhibit the mechanism of fluid secretion by human submandibular salivary acinar cells. Arthritis Rheum 2006; 54:1165–73.

11 Bacman SR, Berra A, Sterin-Borda L, Borda ES. Human primary Sjögren's syndrome autoantibodies as mediators of nitric oxide release coupled to lacrimal gland muscarinic acetylcholine receptors. Curr Eye Res 1998; 17:1135–42.

12 Gao J, Cha S, Jonsson R, Opalko J, Peck AB. Detection of anti-type 3 muscarinic acetylcholine receptor antibodies in the sera of Sjögren's syndrome patients by use of a transfected cell line assay. Arthritis Rheum 2004; 50:2615–21.

13 Marczinovits I, Kovacs L, Gyorgy A *et al.* A peptide of human muscarinic acetylcholine receptor 3 is antigenic in primary Sjögren's syndrome. J Autoimmun 2005; 24:47–54.

14 Kovacs L, Marczinovits I, Gyorgy A *et al.* Clinical associations of autoantibodies to human muscarinic acetylcholine receptor 3[213–228] in primary Sjögren's syndrome. Rheumatology 2005; 44:1021–5.

15 Cavill D, Waterman SA, Gordon TP. Failure to detect antibodies to extracellular loop peptides of the muscarinic M3 receptor in primary Sjögren's syndrome. J Rheumatol 2002; 29:1342–4.

Review

Functional role of M3 muscarinic acetylcholine receptor (M3R) reactive T cells and anti-M3R autoantibodies in patients with Sjögren's syndrome

Takayuki Sumida *, Hiroto Tsuboi, Mana Iizuka, Yumi Nakamura, Isao Matsumoto

Division of Clinical Immunology, Doctoral Program in Clinical Sciences, Graduate School of Comprehensive Human Sciences, University of Tsukuba, 1-1-1 Tennodai, Tsukuba-city, Ibaraki 305-8575, Japan

ARTICLE INFO

ABSTRACT

Sjögren's syndrome (SS) is an autoimmune disease characterized by lymphocytic infiltration into the lachrymal and salivary glands, leading to dry eyes and mouth. Infiltration is also found in the kidneys, lungs, thyroid, and liver. Immunohistochemical studies have shown that most infiltrating lymphocytes are CD4$^+$ T cell receptor (TCR) $\alpha\beta$ T cells. The antigen specificity of T cells is decided by TCR expressed on T cells. The usage of TCRα and TCRβ genes have been examined by immunological and molecular biological methods. Autoantigens recognized by T cells infiltrating into salivary glands have been analyzed and several candidates for autoantigens have been clarified. In the present study, we focused on M3 muscarinic acetylcholine receptor (M3R) as a salivary gland-specific autoantigen and clarified T cell epitopes and B cell epitopes on M3R. The functions of anti-M3R antibodies and M3R reactive T cells were also carried out. To clarify whether M3R reactive T cells play a crucial role in the generation of autoimmune sialoadenitis, splenic CD3 + T cells form M3R$^{-/-}$ mice immunized by M3R peptides were transferred into Rag-1$^{-/-}$ mice and sialoadenitis analyzed. The functional role of M3R reactive T cells in the generation of SS was also discussed.

© 2010 Published by Elsevier B.V.

Contents

1. TCR repertoire of T cells infiltrating into several organs in patients with Sjögren's syndrome

Previous studies with several polymerase chain reaction (PCR) methods, T cell lines, immunofluorescence staining, or flow cytometry analyses provide evidence about the TCR Vβ and Vα genes on T cells in salivary glands, lachrymal glands, kidneys and peripheral blood from patients with Sjögren's syndrome (SS), suggesting the preferential usage of TCR genes. Moreover, the sequence analysis of the CDR3

region indicates some conserved amino acid motifs. These observations support the notion that infiltrating T cells recognize relatively few epitopes on autoantigen [1–15] as shown in Table 1.

2. Autoantigens recognized by T cells in salivary glands from patients with Sjögren's syndrome

Candidate autoantigens recognized by T cells infiltrating the labial salivary glands of patients with SS have been analyzed, and Ro/SSA 52 kDa, α-amylase, heat shock protein, and TCR BV6 [16–18] have been identified. Recently, we have provided evidence for the presence of M3R reactive T cells in peripheral blood of patients with SS [19].

* Corresponding author. Tel.: +81 29 853 3221; fax: +81 29 853 3222.
E-mail address: tsumida@md.tsukuba.ac.jp (T. Sumida).

Table 1
TCR repertoire of T cells infiltrating into several organs in Sjögren's syndrome patients.

TCR repertoire	Methods	Authors	Year	Ref.
A) T cells in salivary glands				
Vβ2/Vβ13	Family PCR	Sumida et al.	1992	[1]
Restricted Jβ	Sequencing	Yonaha et al.	1992	[2]
Vβ5,6,13	Anchored PCR	Dwyer et al.	1993	[3]
Restricted Vβ	T cell lines	Legras et al.	1994	[4]
Conserved CDR3	Sequencing	Sumida et al.	1994	[5]
Limited Vα	Inversed PCR	Sumida et al.	1994	[6]
Vβ2,8	IF	Smith etal.	1997	[7]
Fas-sensitive TCR	SSCP	Sumida et al.	1997	[8]
TCR BV2/AV2	Single cell PCR	Matsumoto et al.	1999	[9]
TCR BV13S2	Quantitative PCR	Kay et al.	1999	[10]
B) T cells in lachrymal glands				
Heterogenous Vβ	Family PCR	Mizushima et al.	1995	[11]
Common TCR	SSCP	Matsumoto et al.	1996	[12]
C) T cell in kidneys				
Vβ2	Family PCR	Murata et al.	1995	[13]
D) Peripheral T cells				
Decreased TCR Vβ6.7a	FC	Kay et al.	1991	[14]
TCR BV13.2	ARMS-PCR	Kay et al.	1995	[15]

3. T cell epitopes on M3R in patients with Sjögren's syndrome

The 25mer synthetic amino acids encoding the second extra-cellular domain of M3R (KRTKVPPGECFIAFLSEPTITFGTAI, AA213-237) were used as the antigen for T cells, and the number of IFN-γ producing T cells was counted by flow cytometry using a magnetic activated cell sorting (MACS) secretion assay. The proportion of IFN-γ producing T cells among peripheral blood mononuclear cells (PBMCs) was high in 40% of primary SS patients with HLA-DR B1*0901 allele. The 25mer amino acids contain the anchored motifs that bind to HLA-DR B1*0901, indicating that KRTKVPPGECFIAFLSEPTITFGTAI should be one of T cell epitopes on M3R molecule [19].

4. B cell epitopes on M3R in patients with Sjögren's syndrome

The presence of autoantibodies (Abs) against M3R has been reported, and it is suggested that an immune reaction to M3R plays a crucial part in the generation of SS [20–22]. Robinson et al. [20] demonstrated that human anti-M3R Abs reduce the secretory function in NOD Igμnull mice. Moreover, Bacman et al. [21] clearly showed that human anti-M3R Abs against the second extra-cellular loop of M3R could activate nitric oxide synthetase coupled to the lachrymal gland M3R, suggesting that anti-M3R Abs are a new marker of dry eye SS. The M3Rs are expressed on salivary and lachrymal glands, and thus they should be key receptors involved in the production of saliva and tears after stimulation of acetylcholine. Thence, autoAbs against M3R could interfere with the production of saliva and tears. We analyzed the prevalence of anti-M3R Abs in adult patients with SS and child-onset SS [23,24]. Recently, B cell epitopes recognized by anti-M3R Abs in 42 patients with SS have been examined using synthetic peptides encoding N-terminal region, the first extra-cellular domain, the second extra-cellular domain, and the third extra-cellular domain by ELISA method. Abs to the N-terminal, the first, second and third extra-cellular domains were detected in 42.9% (18/42), 47.6% (20/42), 54.8% (23/42), and 45.2% (19/42) of SS, while in 4.8% (2/42), 7.1% (3/42), 2.4% (1/42), and 2.4% (1/42) of controls, respectively (Tsuboi, et al. personal data). Results were summarized in Table 2. These findings indicated the presence of several B cell epitopes on M3R in SS.

5. Function of anti-M3R Abs in patients with SS

For functional analysis, human salivary gland (HSG) cells were pre-incubated with IgG separated from sera of anti-M3R Abs-positive

Table 2
B cell epitopes on M3R and function of anti-M3R antibodies in patients with Sjögren's syndrome (SS).

B cell epitopes					
N region	First ECD	Second ECD	Third ECD		
+	+	+	+	50	
+	−	+	+	3.6	
−	+	+	+	3.6	
+	+	−	−	3.6	
+	−	+	−	3.6	
−	+	+	−	7.1	
−	+	+	+	7.1	
+	−	−	−	3.6	Enhancement
−	+	−	−	7.1	Enhancement
−	−	+	−	7.1	Suppression
−	−	−	+	3.6	No effect

ECD, extra-cellular domain.

SS, -negative SS, and controls for 12 h. After loading with Fluo-3, HSG cells were stimulated with cevimeline hydrochloride, and intracellular Ca^{2+} concentrations ($[Ca^{2+}]i$) were measured. Abs to the second extra-cellular domain positive SS-IgG inhibited the increase of $[Ca^{2+}]i$ induced by cevimeline hydrochloride. Abs to the N-terminal positive SS-IgG and Abs to the first extra-cellular domain positive SS-IgG enhanced it, while Abs to the third extra-cellular domain positive SS-IgG showed no effect on $[Ca^{2+}]i$ as well as anti-M3R Abs negative SS-IgG (Tsuboi, et al. submitting). The results were shown in Table 2. Our functional data suggested that the influence of anti-M3R Abs on salivary secretion might differ based on these epitopes.

6. M3R reactive T cells are essential for the generation of autoimmune sialoadenitis

To clarify the role of the immune response to M3R in the pathogenesis of SS, $M3R^{-/-}$ mice were immunized with murine M3R peptides and their splenocytes were inoculated into $Rag1^{-/-}$ ($M3R^{-/-} \to Rag1^{-/-}$) mice. Anti-M3R Abs were increased in sera and saliva volume was decreased in $M3R^{-/-} \to Rag1^{-/-}$ mice. Histological examination showed marked infiltration of mononuclear cells in the salivary glands and immunohistochemistry demonstrated that the majority of these cells were CD4+ T cells with a few B cells and several IFN-γ- and IL-17-producing cells. Apoptotic cells were present in the salivary glands of $M3R^{-/-} \to Rag1^{-/-}$ mice. Moreover, transfer of only CD3+ T cells from $M3R^{-/-}$ immunized with M3R peptides into $Rag1^{-/-}$ mice resulted in cell infiltration and destruction of epithelial cells in the salivary glands, suggesting that M3R reactive CD3+ T cells play a pathogenic role in the development of autoimmune sialoadenitis (Fig. 1) (Iizuka et al, submitting). Our findings support the notion

Fig. 1. Histological analysis of salivary glands isolated from $M3R^{-/-} \to Rag1^{-/-}$ mice. Salivary glands isolated from $Rag1^{-/-}$ mice at day 45 after inoculation of splenocytes from immunized $M3R^{-/-}$ and $M3R^{+/+}$ mice. Salivary glands were sectioned at 4 μm, and each section was stained with Mayer's hematoxylin and eosin (H&E).

that M3R reactive immune reaction plays a crucial role in the pathogenesis of SS-like autoimmune sialoadenitis.

Take-home messages

* Anti-M3R Abs were detected in 50% of Sjögren's Syndrome (SS) patients, suggesting the possible serological marker for diagnosis of SS.
* The functional difference among anti-M3R antibodies against distinct B cell epitopes should shed light on the pathogenic roles of anti-M3R Abs in salivary secretion abnormalitites in SS patients.
* Murine model for autoimmune sialoadenitis using M3R$^{-/-}$ → Rag-1$^{-/-}$ mice clearly showed that M3R reactive T cells play a crucial role in the generation of SS-like autoimmune sialoadenitis.

References

[1] Sumida T, Yonaha F, Maeda T, Tanabe E, Koike T, Tomioka H, et al. T cell receptor repertoire of infiltrating T cells in lips of Sjögren's syndrome patients. J Clin Invest 1992;89:681–5.

[2] Yonaha F, Sumida T, Maeda T, Tomioka H, Koike T, Yoshida S. Restricted junctional usage of T cell receptor Vβ2 and Vβ13 genes, which are overrepresented on infiltrating T cells in the lips of patients with Sjögren's syndrome. Arthritis Rheum 1992;35:1362–7.

[3] Dwyer E, Itescu S, Winchester R. Characterization of the primary structure of T cell receptor β chains in cells infiltrating the salivary gland in the sicca syndrome of HIC-1 infection. J Clin Invest 1993;92:495–502.

[4] Legras F, Martin T, Knapp AM, Pasquali JL. Infiltrating T cells from patients with primary Sjogren's syndrome express restricted or unrestricted T cell receptor Vβregions depending on the stage of the disease. Eur J Immunol 1994;24:181–5.

[5] Sumida T, Skamaki T, Yonaha F, Maeda T, Namekawa T. Nawata, et al. LA-DR alleles in patients with Sjogren's syndrome over-representing Vβ2 and Vβ13 genes in the salivary glnads. Br J Rheumatol 1994;33:420–4.

[6] Sumida T, Kita Y, Yonaha F, Maeda T, Iwamoto I, Yoshida S. T cell receptor Vα repertoire of infiltrating T cells in labial salivary glands from patients with Sjogren's syndrome. J Rheumatol 1994;21:1655–61.

[7] Smith MD, Lamour A, Boylston A, Lancaster FC, Pennec YL, van Agthoven A, et al. Selective expansion of Vβ families by T cells in the blood and salivary gland infiltrate of patients with primary Sjögren's syndrome. J Rheumatol 1994;21: 1832–7.

[8] Sumida T, Matsumoto I, Murata H, Namekawa T, matsumura T, Tomioka H, et al. TCR in Fas-sensitive T ells from labial salivary glands of patients with Sjogren's syndrome. J Immunol 1997;158:1020–5.

[9] Matsumoto I, Okada S, Kuraoda K, Iwamoto I, Saito Y, Tokuhisa T, et al. Single cell analysis of T cells infiltrating labial salivary glands from patients with Sjogren's syndrome. Int J Mol Med 1999;4:519–27.

[10] Furrie E, Doherty M, Kershaw A, Crighton A, Morley K, Kay R. Molecular evidence of antigen-driven Vβ13.2 T cells in the lip biopsies and peripheral blood of anti-52 kDa Ro autoantibody positive Sjogren's syndrome patients. Arthritis Rheum 1999;S403.

[11] Mizushima N, Kohsaka H, Tsubota K, Saito I, Miyasaka N. Diverse T cell receptor β gene usage by infiltrating T cells in the lacrimal glands of Sjogren's syndrome. Clin Exp Immunol 1995;101:33–8.

[12] Matsumoto I, Tsubota K, Satake Y, Kita Y, Matsumura R, Murata H, et al. Common T cell receptor clonotype in lacrimal glands and labial salivary glands of patients with Sjögren's syndrome. J Clin Invest 1996;97:1969–77.

[13] Murata H, Kita Y, Sakamoto A, Matsumoto I, Matsumura R, Sugiyama T, et al. Limited T cell receptor repertoire of infiltrating T cells in the kidneys of Sjögren's syndrome patients with interstitial nephritis. J Immunol 1995;155:4084–9.

[14] Kay RA, Hay EM, Dyer PA, Dennett C, Green LM, Bernstein RM, et al. An abnormal T cell repertoire in hypergammaglobulinemic primary Sjogren's syndrome. Clin Exp Immunol 1991;85:262–4.

[15] Kay RA, Hutchings CJ, Ollier WER. A subset of Sjögren's syndrome associates with the TCRBV13S2 locus but not the TCRBV2S1 locus. Hum Immunol 1995;42: 328–30.

[16] Sumida T, Namekawa T, Maeda T, Nishioka K. New T cell epitope of Ro/SS-A 52 kDa protein in labial salivary glands from patients with Sjogren's syndrome. Lancet 1996;348:1667.

[17] Sumida T, Kato T, Hasunuma T, Maeda T, Nishioka K, Matsumoto I. Regulatory T cell epitope recognized by T cells from labial salivary glnads of patients with Sjögren's syndrome. Arthritis Rheum 1997;40:2271–3.

[18] Matsumoto I, Maeda T, Takemoto Y, Hashimoto Y, Kimura F, Iwamoto I, et al. α-amylase functions as a salivary gland-specific self T cell epitope in patients with Sjögren's syndrome. Int J Mol Med 1999;3:485–90.

[19] Naito Y, Matsumoto I, Wakamatsu E, Goto D, Ito S, Tsutsumi A, et al. Altered peptide ligands regulate muscarinic acetylcholine receptor reactive T cells of patients with Sjogren's syndrome. Ann Rheum Dis 2005;65:269–71.

[20] Robinson CP, Brayer J, Yomochika S, Esch TR, Peck AB, Stewart CA, et al. Transfer of human serum IgG to nonobese diabetic Igμnull mice reveals a role for autoantibodies in the loss of secretory function of exocrine tissues in Sjogren's syndrome. Proc Natl Acad Sci USA 1998;95:7538–43.

[21] Bacman S, Berro A, Sherrin-Borda I, Borda E. Muscarinic acetylcholine receptor antibodies as a new marker of dry eye Sjögren's syndrome. Invest Opthalmol Cis Sc 2001;42:321–7.

[22] Nguyen K, Broyer J, Cha S, Diggs S, Yosunori U, Hilal G, et al. Evidence for anti-muscarinic acetylcholine receptor antibody-mediated secretory dysfunction in NOD mice. Arthritis Rheum 2000;43:2297–306.

[23] Naito Y, Matsumoto I, Wakamatsu E, Goto D, Sugiyama T, Matsumura R, et al. Muscarinic acetylcholine receptor autoantibodies in patients with Sjögren's syndrome. Ann Rheum Dis 2005;64:510–1.

[24] Nakamura Y, Wakamatsu E, Matsumoto I, Tomiita M, Kohno Y, Mori M, et al. High prevalence of autoantibodies to muscarinic-3 acetylcholine receptor in patients with juvenile-onset Sjögren's syndrome. Ann Rheum Dis 2008;67:136–7.

Indirect inhibition of in-vivo and in-vitro T-cell responses by intravenous immunoglobulins due to impaired antigen presentation

Several clinical studies done with intravenous immunoglobulin (IVIg)-treated autoimmune patients as well as several in vitro studies have revealed that IVIg can reduce polyclonal T-cell activation and modify their cytokine secretion pattern. However, their effect on auto-antigen-specific T-cell responses has never been addressed directly. In the present study, **Aubin E. et al. (Blood 2010; 115: 1727-34)** used an in vivo model of induction of antigen-specific T-cell responses and an in vitro antigen presentation system to study the effects of IVIg on T-cell responses. The results obtained showed that IVIg inhibited both the in vivo and in vitro antigen-specific T-cell responses but that this effect was the indirect consequence of a reduction in the antigen presentation ability of antigen=presenting cells. The inhibitory effect of IVIg was FcgammaRIIb-independent, suggesting that IVIg must interfere with activating FcgammaRs expressed on antigen-presenting cells to reduce their ability to present antigens. Such inhibition of T-cell responses by reducing antigen presentation may therefore contribute to the well-known anti-inflammatory effects of IVIg in autoimmune diseases.

Rituximab treatment overcomes reduction of regulatory iNKT cells in patients with rheumatoid arthritis

Invariant natural killer T (iNKT) cells are subset of T cells that recognize glycolipid antigens presented by the CD1d molecule. Accumulating evidences showed that iNKT cells are implicated in the regulatory mechanisms that control autoimmunity. Here, Parietti V. et al. (Clin Immunol 2010; 134: 331-9) evaluated the number of circulating iNKT cells in patients with rheumatoid arthritis (RA) by flow cytometry and performed a longitudinal analysis of iNKT cell frequency in RA patients who were given an anti-CD20 therapy. Significantly lower iNKT cell numbers were measured in the blood from RA patients compared to healthy individuals (p < 0.0001) and low iNKT cell frequencies were rather associated with an active disease. In RA patients who received rituximab treatment, iNKT cell number was increased in relation to the clinical outcome. Thus, it was demonstrated that the number of iNKT cells is altered in RA patients and that following rituximab therapy, clinical remission of RA is associated with an increase of iNKT cell frequency.

Induction of T$_h$1-biased cytokine production by α-carba-GalCer, a neoglycolipid ligand for NKT cells

Takuya Tashiro[1], Etsuko Sekine-Kondo[1], Tomokuni Shigeura[1], Ryusuke Nakagawa[1], Sayo Inoue[1], Miyuki Omori-Miyake[1], Tomoki Chiba[1], Naomi Hongo[1], Shin-ichiro Fujii[2], Kanako Shimizu[2], Yohei Yoshiga[3], Takayuki Sumida[3], Kenji Mori[1], Hiroshi Watarai[1] and Masaru Taniguchi[1]

[1]Laboratory for Immune Regulation and [2]Research Unit for Cellular Immunotherapy, RIKEN Research Center for Allergy and Immunology, Tsurumi, Yokohama, Japan
[3]Department of Internal Medicine, Tsukuba University, Tsukuba, Ibaraki, Japan

Correspondence to: M. Taniguchi; E-mail: taniguti@rcai.riken.jp

Transmitting editor: M. Miyasaka

Received 29 May 2009, accepted 22 January 2010

Abstract

NKT cells are characterized by their production of both T$_h$1 and T$_h$2 cytokines immediately after stimulation with α-galactosylceramide (α-GalCer), which is composed of α-galactopyranose linked to ceramide (itself composed of sphingosine and fatty-acyl chains); the chain length of the ceramide varies and this affects the ability of α-GalCer to stimulate cytokine production. However, the contribution of its galactopyranose sugar moiety remains unclear. We synthesized α-carba-GalCer, which has α-linked carba-galactosyl moiety; here, the 5a'-oxygen atom of the α-galactopyranose ring of α-GalCer is replaced by a methylene group. The α-carba-GalCer was more stable and showed higher affinity to the NKT receptor. It thus enhanced and prolonged production of IL-12 and IFN-γ compared with α-GalCer, resulting in augmented NKT cell-mediated adjuvant effects in vivo. The α-carba-GalCer, which has an ether linkage, was more resistant to degradation by liver microsomes than was α-GalCer, which has an acetal bond. Modulation of the sugar moiety in glycolipids might therefore provide optimal therapeutic reagents for protective immune responses against tumor or pathogens.

Keywords: CD1d, glycolipid, IFN-γ, NKT cells, TCR

Introduction

NKT cells express an invariant TCRα chain encoded by a Vα14-Jα18 or a Vα24-Jα18 gene in mice (1) or humans (2, 3), respectively. NKT cells recognize CD1d-restricted glycolipids, such as α-galactosylceramide (α-GalCer), and rapidly produce T$_h$1 cytokines, for example IFN-γ, and T$_h$2 cytokines, for example IL-4 (1). NKT cell production of IFN-γ mediates strong adjuvant effects for protective anti-tumor immune responses because of IFN-γ-mediated activation of NK cells and CD8$^+$ killer T cells (4–6). On the other hand, T$_h$2 cytokine production, such as IL-10, enhances regulatory immune responses and prevents development of certain autoimmune diseases (7, 8). Thus, it has long been thought desirable to regulate the function of NKT cells by using optimized glycolipid ligands, for example by modulating the ceramide or sugar moieties, which would possibly increase the stability of the TCR–CD1d–glycolipid triple complex.

The antigen-binding sites of mouse and human CD1d molecules are composed of two large hydrophobic pockets, designated A' and F', that can accommodate the fatty-acyl

chain and the sphingosine chain of ceramide, respectively (9, 10). Up to 26 carbon atoms of the acyl chain can be anchored on the A' pocket, whereas 18 carbon atoms are anchored on the F' pocket. We have previously shown that glycolipids with these lengths of alkyl chains are the most effective in stimulating NKT cells (11), suggesting that the optimized alkyl chain lengths lead the most stable association with CD1d molecule and the production of both T$_h$1 and T$_h$2 cytokines. McCarthy et al. (12) have also shown that the lengths and saturation of both alkyl chains affect the stability of binding to CD1d, resulting in a modulated NKT cell TCR-binding affinity and immunological synapse formation. Furthermore, it has been reported that OCH (an α-GalCer analogue with a truncated sphingosine chain) induces T$_h$2-biased cytokine production because of the low affinity of OCH to CD1d (13). OCH has been shown to diminish NKT cell IFN-γ production and CD40 ligand (CD40L) expression because of the failure of antigen-presenting cells (APC) to produce IL-12 (14). On the basis of these findings, the

stability of the CD1d–glycolipid complex has been considered to be the major factor that could evoke the shifted cytokine production by affecting the association of glycolipids with the CD1d molecule.

The above-mentioned hydrophobic interactions of the alkyl chains on α-GalCer affect its structure and function as a glycolipid ligand. Recent studies on crystal structures have revealed that the 3-hydroxyl group on the sphingosine chain and the 2-hydroxyl group on the D-galactopyranose moiety of α-GalCer bind to form hydrogen bonds with Arg95 and Gly96, respectively, in the complementarity-determining region (CDR) 3 of the human invariant NKT TCR Vα24Jα18 (9). These findings suggest that the sugar moiety is also important to make a stable NKT TCR–α-GalCer–CD1d complex. Therefore, in the generation of neoglycolipids with desired NKT cell function, it is necessary to consider structural modification of the sugar moiety of the NKT cell ligands.

Here, we demonstrated that a new synthetic α-GalCer analogue, α-carba-GalCer, in which the 5a′-oxygen atom of the pyranose ring of D-galactose is replaced by a methylene group, evoked a potent T_h1-biased response and augmented NKT cell-mediated adjuvant effects in vivo. Since α-carba-GalCer has a stable ether linkage, it is likely to be resistant to galactosidase and thus be structurally stable in vivo. Moreover, the replacement of the O atom of D-galactose by a CH_2 group generated a new hydrophobic interaction with Pro28 on CDR1 of the invariant NKT TCRα chain, resulting in their stable interaction.

Methods

Mice

Specific pathogen-free C57BL/6 (B6) mice were purchased from Charles River (Kanagawa, Japan) and $TAP^{-/-}$ B6 mice were kept under specific pathogen-free conditions and used at 8–16 weeks of age. All experiments were in accordance with protocols approved by RIKEN Animal Care and Use Committee.

Reagents

The α-carba-GalCer was synthesized as described previously (15). One milligram of α-carba-GalCer was dissolved in dimethyl sulfoxide and diluted with saline to adjust the concentration to 200 μg ml⁻¹. The α-GalCer was purchased from Funakoshi (Tokyo, Japan). LPS-free ovalbumin (OVA) was from Seikagaku Corp. (Tokyo, Japan). Analysis of cell surface markers or intracellular cytokine staining and cell sorting was performed using the following mAb or recombinant proteins in FACS analysis: fluorescent isothiocyanate (FITC) anti-TCRβ (H57-297), mouse CD1d–mouse IgG1 fusion protein (Dimer X), APC-conjugated anti-mouse IgG1 (X56), allophycocyanin anti-mouse CD11c (HL3), phycoerythrin (PE) anti-mouse IL-12 (C15.6), FITC anti-mouse CD8α (53-6.7), peridinin-chlorophyll protien-Cy5.5 B220 (RA3-6B2), APC anti-mouse IFN-γ (XMG1.2) (BD Biosciences, San Diego, CA, USA), PE anti-human Vα24 TCR (C15), FITC anti-human Vβ11 TCR (C21) and Pacific Blue anti-human CD4 (RPA-T4) (eBioscience, San Diego, CA, USA). The α-carba-GalCer or α-GalCer-loaded CD1d dimers were pre-pared as described previously (16). For in vivo neutralizing experiments, goat polyclonal IgG specific for anti-mouse IL-12 and anti-mouse CD40L was used and purchased from R&D systems (Minneapolis, MN, USA).

Cytokine measurement

The cytokine concentrations in plasma or culture supernatants were quantified by a cytometric bead array (BD Bioscience) and mouse IFN-γ ELISA kit (Thermo Scientific Endogen, Rockford, IL, USA) according to the manufacturer's protocol.

Flow cytometry and cell sorting

Spleen or liver mononuclear cells (MNCs) from mice and PBMCs from human healthy volunteers were isolated as described previously (16). Flow cytometry was performed using a FACSCalibur and CELLQuest (BD Biosciences) or FACSAria and FACSDiVa (BD Biosciences). FlowJo software (Tree Star, Ashland, OR, USA) was used for analysis; all the data were live gated based on forward and side scatter and propidium iodide exclusion. For isolation, cells were sorted by an FACSDiVa and FACSAria (BD Biosciences), and the purity of sorted cells was usually >99%.

Intracellular cytokine staining

Intracellular cytokine staining was performed as described previously (16). For IL-12 in whole spleen cells or dendritic cells (DCs), and IFN-γ in CD8⁺ T cells, Brefeldin A (Sigma-Aldrich, St Louis, MO, USA) was added for the last 4–5 h of culture to accumulate intracellular cytokines. Cells were then washed and incubated with anti-mouse CD11c mAb for whole spleen cells or anti-mouse CD8 mAb for CD8⁺ T cells for 20 min at 4°C after first blocking the Fc receptors with an anti-CD16/CD32 antibody. Following fixation with Cytofix/Cytoperm plus™ (BD Biosciences), cells were stained for intracellular IFN-γ for 15 min at room temperature.

Adjuvant activity of ligand-activated NKT cells on OVA-specific CD8⁺ T cells

The adjuvant activities of NKT cells were assayed as described previously (5). Briefly, spleen cells from $TAP^{-/-}$ mice were incubated with hypertonic medium in the presence of 10 mg ml⁻¹ OVA and then incubated with hypotonic medium to induce apoptosis. This cell-associated form of OVA was injected intravenously (2 × 10⁷ cells per mouse) together with α-GalCer or α-carba-GalCer (2 μg per mouse) into B6 wild-type mice on a B6 background. After 7 days, spleen cells were stimulated in vitro with 1 μM OVA₂₅₇₋₂₆₄ peptide for 6 h and then IFN-γ production by CD8⁺ T cells was monitored by intracellular staining.

NK cell-mediated cytotoxicity

NK cell-sensitive YAC-1 lymphoma cells were used as target cells. Target cells (2 × 10⁶) were labeled for 60 min at 37°C with 100 μCi of Na⁵¹CrO₄ in 200 μl of serum. Then, they were washed three times with medium and subjected to a cytotoxicity assay. Labeled target cells (2 × 10³ cells per well) were incubated with spleen cells or liver MNCs (prepared

from B6 mice) previously treated with ligands for 4 h at 37°C in 96-well round-bottom plates. The plates were then centrifuged, the resulting supernatants were harvested and their content of radioactivity was determined with a gammacounter (PerkinElmer, Waltham, MA, USA).

In vitro stimulation of mouse NKT cells

Bone marrow-derived DCs (BMDCs) were raised from bone marrow precursors in the presence of granulocyte macrophage colony-stimulating factor (GM-CSF) (5 µg ml^{-1}) for 6 days (17) and were incubated with either glycolipid α-GalCer or α-carba-GalCer for 2 h in a 37°C CO$_2$ incubator before co-culture with NKT cells. After washing the glycolipid-loaded BMDCs in ice-cold RPMI1640 medium (with 2% FCS) three times, 0.2 million NKT cells were isolated by FAC-SAria (Beckton Dickinson), at a purity of >99%, and were seeded onto the glycolipid-pulsed BMDCs in a total volume of 200 µl and co-cultured for the indicated times. In the case of blocking experiments, NKT cells were incubated with anti-CD40L mAb (clone MR1, BD Biosciences) before the addition of BMDCs for 30 min in a 37°C CO$_2$ incubator. Similarly, BMDCs were incubated with anti-IL-12 receptor β2 mAb (clone HAM10B9, BD Biosciences) before the addition of NKT cells. All *in vitro* stimulations of NKT cells were performed in a 37°C CO$_2$ incubator for the indicated times.

Surface plasmon resonance

The affinity and kinetic properties of 'invariant' Vα14/Vβ8.2 binding to α-carba-GalCer–CD1d or α-GalCer–CD1d complexes were measured with a spectrometer (model3000, Biacore, Buckinghamshire, UK) as previously described (18). The recombinant CD1d loaded with α-carba-GalCer or α-GalCer was immobilized onto CM5 sensor chips (Biacore) at a level of 1000 resonance units. In all experiments, glycolipid-unloaded CD1d was used as a negative control. Equilibrium binding was performed at a flow rate of 10 µl min^{-1} from the lowest concentration of Vα14/Vβ8.2. Equilibrium dissociation constants (K_d) values were calculated using the standard hyperbolic model. The kinetics of the Vα14/Vβ8.2–CD1d–glycolipid interactions were measured at 50 µl min^{-1}. K_d, k_{on} and k_{off} were obtained by non-linear curve fitting of the binding curves obtained after subtracting the response in the reference flow cells with equations derived from the simple 1:1 Langmuir-binding model using the biosensor immunoassays evaluation program (version 3.02.2; Biacore).

Analysis of glycolipid stability

The α-GalCer (100 ng) or α-carba-GalCer (100 ng) was incubated with mouse liver microsomes (50 µg) (BD) for 24 or 48 h at 37°C. Glycolipids were recovered by extraction with chloroform and used for stimulation of whole spleen cells to analyze IFN-γ production.

In vitro stimulation of human PBMCs

Human PBMCs from healthy volunteers were prepared as previously described (16). CD14$^+$ monocytes were positively selected by MACS (Miltenyi Biotech, Bergisch Gladbach, Germany) and CD14$^-$ PBMCs were stored at −80°C for 5

days. Monocyte-derived DCs (MoDCs) were generated from CD14$^+$ monocytes by culturing with GM-CSF (50 ng ml^{-1}) and IL-4 (100 ng ml^{-1}) for 5 days. After generation of DCs, CD14^{-1} PBMCs (10^5 cells per 100 µl) were co-cultured with MoDCs (10^4 cells per 100 µl) in the presence or absence of glycolipid and NKT cell expansion and cytokine production were analyzed.

Statistics

Data are presented as mean values ± SD. Student's *t*-test was used to determine statistical significance between groups, with $P < 0.05$ being considered significant.

Results

Synthesis of a neoglycolipid, α-carba-GalCer, by the replacement of the 5a'-oxygen atom of the pyranose ring of D-galactose on α-GalCer by a methylene group

According to the crystal structure of α-GalCer–CD1d (9, 19), the glycosidic oxygen atom of α-GalCer makes a hydrogen bond with CD1d (mouse: Thr156 and human: Thr154) and plays an important role in making a stable complex. In addition, it is known that the ether-linked analogue of α-GalCer, α-C-GalCer, induces T_h1-biased cytokine production (20). On the basis of these results, we synthesized a carbocyclic analogue, α-carba-GalCer (Fig. 1), with a linking oxygen atom and hence an ether linkage. A detailed procedure for synthesis of α-carba-GalCer has already been reported (15). The synthetic α-carba-GalCer possesses all the hydroxyl groups of α-GalCer, so that it satisfies the structural requirements for making the complex with the NKT TCR and CD1d.

α-carba-GalCer exhibits enhanced T_h1-biased cytokine production in vivo

The staining profiles of NKT cells with α-carba-GalCer were first investigated by α-carba-GalCer-loaded soluble recombinant CD1d according to the protocols published (21–23). The α-carba-GalCer-loaded CD1d dimer stained mouse NKT cells, similarly to those stained with an α-GalCer-loaded CD1d dimer (Fig. 2A). To examine the functional activity of α-carba-GalCer, we administered α-carba-GalCer or α-GalCer intravenously and monitored serum cytokine levels (Fig. 2B and C). The administration of α-carba-GalCer (2 µg) resulted in enhanced and long-lasting production of IFN-γ, which peaked at 36 h after stimulation, whereas IFN-γ production by α-GalCer peaked at 12 h (Fig. 2C). IL-12p70, which is important for production of IFN-γ, also showed prolonged and enhanced production after α-carba-GalCer administration compared with α-GalCer (Fig. 2C). On the other hand, the α-carba-GalCer-stimulated production of other cytokines, such as IL-4 or IL-13, IL-2 and IL-17A, was transient, which was similar to the findings with α-GalCer (Fig. 2B and C). It is interesting that a second wave of cytokine production was observed for IL-10, tumor necrosis factor (TNF)-α and GM-CSF, which peaked at ~36 h after treatment with α-carba-GalCer and α-GalCer. However, the significant augmentation of the second wave was observed only for IL-10 and TNF-α but not GM-CSF after treatment with α-carba-GalCer rather than α-GalCer (Fig. 2B).
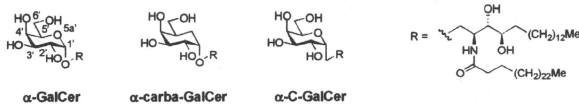
α-GalCer   α-carba-GalCer   α-C-GalCer

Fig. 1. Structure of α-GalCer, α-carba-GalCer and α-C-GalCer. The difference between α-GalCer and α-carba-GalCer is the replacement of the 5a'-oxygen atom of the pyranose ring of D-galactose (5a'-O) by a methylene group. The structure of α-C-GalCer with a C-glycosidic (ether) linkage to the ceramide portion is also shown for their comparison. The ceramide moiety (R) of these glycolipids is also illustrated.

Mechanisms of T_h1-biased cytokine production by α-carba-GalCer in vitro

The IL-12p70 production by DCs and subsequent IFN-γ production by NKT cells after α-GalCer stimulation are largely dependent on the interaction between CD40L on NKT cells and CD40 on DCs (24). Thus, we intraperitoneally administered either anti-IL12 or anti-CD40L 1 day before injection of either α-GalCer or α-carba-GalCer (Fig. 3A and B). As expected, either blocking of CD40–CD40L interaction or neutralization of IL-12 resulted in suppression of IL-12 and IFN-γ production, indicating that the mechanisms of adjuvant effects induced by α-carba-GalCer are based on the IL-12-initiated augmented IFN-γ production, similar to those by α-GalCer.

We then tested which cell types are responsible for α-carba-GalCer-mediated IL-12 production. Spleen cells were collected 1 h after α-GalCer or α-carba-GalCer administration, cultured for 5 h *in vitro* and analyzed for IL-12-producing cells by intracellular cytokine staining. Both α-GalCer and α-carba-GalCer led to IL-12 production from CD11c+ DCs (Fig. 3C). Furthermore, the ratio of IL-12-producing DCs was higher in DCs from α-carba-GalCer-injected mice (1.22%) than those from those given α-GalCer (0.85%) (Fig. 3C).

We then asked which DC subsets are responsible for IL-12 production. CD11c+ DCs in Fig. 3C were further divided into CD8α− conventional DCs (CDCs), CD8α+ CDCs and B220+ plasmacytoid DCs (PDCs) on the basis of expression of CD8α and B220. IL-12 was mainly produced from CD8α+ CDC rather than CD8α− CDCs or PDCs (Fig. 3D). We also observed a significant number of IL-12-producing CD11c+CD8α+ CDCs by administration of α-carba-GalCer rather than α-GalCer (Fig. 3D).

To confirm the mechanisms of the production of IL-12 and subsequent IFN-γ, we co-cultured freshly isolated splenic NKT cells with α-GalCer-pulsed or α-carba-GalCer-pulsed GM-CSF-induced BMDCs, which phenotypically and functionally resemble to CD8α+ CDCs. The α-carba-GalCer-pulsed DCs produced higher amounts of IL-12p70 compared with those pulsed with α-GalCer and induced augmented IFN-γ production by NKT cells (Fig. 3E). Moreover, IL-12 and IFN-γ production stimulated *in vitro* by α-carba-GalCer was blocked by either anti-CD40L or anti-IL-12Rβ2 mAbs (Fig. 3E), indicating that augmented IFN-γ production is dependent on CD40–CD40L interaction and augmented IL-12 production.

NKT cell-mediated adjuvant effects on NK and antigen-specific CD8+ T cells after α-carba-GalCer stimulation in mice

We previously demonstrated that the NKT cell production of IFN-γ mediates adjuvant effects, which augment the cyto-

toxic activity of innate NK cells and also increase in the number of IFN-γ-producing CD8+ cytotoxic T cells in the acquired immune system (4, 5). Therefore, we examined the cytotoxicity of mouse liver MNCs or spleen cells from mice treated 4 days previously with α-GalCer or α-carba-GalCer. The liver MNCs of α-carba-GalCer-treated mice exhibited apparently a higher magnitude of cytotoxicity than α-GalCer at any effector:target ratios (Fig. 4A). Also, we observed significant expansion (>2-fold) of IFN-γ-producing OVA-specific CD8+ T cells by co-administration of α-carba-GalCer with OVA-loaded splenocytes, rather than α-GalCer (Fig. 4B).

Affinity measurement of the α-carba-GalCer–CD1d complex to soluble NKT TCR

We measured the affinity of Vα14/Vβ8 binding to the CD1d–glycolipid complex according to the previous studies (11, 24, 25). Purified invariant Vα14 and Vβ8.2 recombinant proteins were used for surface plasmon resonance analysis against immobilized α-carba-GalCer–CD1d or α-GalCer–CD1d. We observed similar affinity with α-GalCer–CD1d (K_d of 84.3 nM, Fig. 5A, upper panel) to those reported previously (12). On the other hand, the affinity of the invariant Vα14/Vβ8.2 to α-carba-GalCer–CD1d (K_d of 44.9 nM, Fig. 5A, lower panel) was slightly higher than that for α-GalCer–CD1d. Comparison of the binding kinetics of invariant Vα14/Vβ8.2 demonstrated that the increase in the affinity observed in α-carba-GalCer–CD1d was as much the result of increases in the k_{on} as decreases in the k_{off} (Fig. 5B).

Stability of α-carba-GalCer

Since α-carba-GalCer has an ether linkage (like α-C-GalCer) instead of the glycosyl (acetal) bond of α-GalCer, it is considered to be resistant to α-glycosidase or hydrolytic enzymes. To test this possibility, we carried out an in vitro microsome assay. Cytochrome P450 (CYP) plays an important role in the oxidative metabolism of numerous endogenous and foreign compounds (26). Because of manifold actions of CYP, we used mouse liver microsomes for treatment of α-carba-GalCer or α-GalCer *in vitro* to analyze their stability. In this experiment, we first generated the standard curves that were based on the amounts of IFN-γ produced after stimulation of spleen cells with untreated glycolipids. According to the standard curve, we calculated a half-life of the glycolipids by measuring IFN-γ production at different time points upon stimulation with the residual glycolipids with assumed concentrations after treatment with liver microsomes (Fig. 5C). The half-life of α-carba-GalCer was ~40 h, which was twice as long as that of α-GalCer (20–25 h), suggesting that α-carba-GalCer is more stable than α-GalCer in terms of hydroxylation.
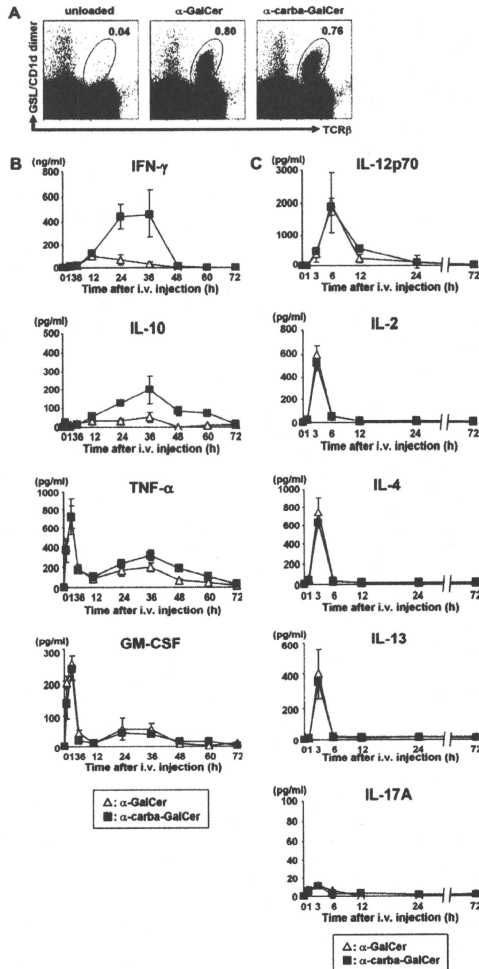
Fig. 2. Analysis of cytokine production mediated by α-carba-GalCer stimulation. (A) Staining of mouse NKT cells by unloaded, α-GalCer-loaded or α-carba-GalCer-loaded CD1d dimers. NKT cells in the spleen were identified by their expression of TCRβ and reactivity with the glycolipid-loaded or -unloaded CD1d dimers (*n* = 3). (B and C) Long-lasting (IFN-γ, IL-10, TNF-α and GM-CSF) (B) and transient (IL-12p70, IL-4, IL-13, IL-2 and IL-17A) (C) production of cytokines induced after intravenous injection of α-carba-GalCer (closed square, 2 µg) or α-GalCer (open triangle, 2 µg). Cytokine levels in sera were measured by ELISA or the cytometric bead array system at the indicated time points. Data are means ± SDs from three mice and repeated three times with similar results.